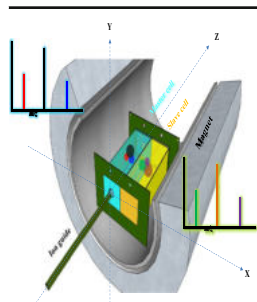


RESEARCH ARTICLE

Parallel Spectral Acquisition with Orthogonal ICR Cells

Sung-Gun Park,¹ Gordon A. Anderson,² James E. Bruce¹¹Department of Genome Sciences, University of Washington, Seattle, WA 98109, USA²GAA Custom Engineering, LLC, Benton City, WA 99320, USA

Abstract. FT-based high performance mass analyzers yield increased resolving power and mass measurement accuracy, yet require increased duration of signal acquisition that can limit many applications. The implementation of stronger magnetic fields, multiple detection electrodes for harmonic signal detection, and an array of multiple mass analyzers arranged along the magnetic field axis have been used to decrease required acquisition time. The results presented here show that multiple ion cyclotron resonance (ICR) mass analyzers can also be implemented orthogonal to the central magnetic field axis. The orthogonal ICR cell system presented here consisting of two cells (master and slave cells) was constructed with printed circuit boards and installed within a single superconducting magnet and vacuum system. A

master cell was positioned, as is normally done with ICR cells, on the central magnetic field axis and a slave cell was located off this central axis, but directly adjacent and alongside the master cell. To achieve ion transfer between cells, ions that were initially trapped in the master cell were drifted across the magnetic field into the slave cell with application of a small DC field applied perpendicularly to the magnetic field axis. A subsequent population of ions was injected and accumulated in the master cell. Simultaneous excitation of cyclotron motion of ions in both cells was carried out; ICR signals from each cell were independently amplified and recorded in parallel. Presented here are the initial results of successful parallel spectral acquisition with this orthogonal dual ICR cell array.

Keywords: FT-ICR, FTMS, Array

Received: 23 September 2016/Revised: 21 November 2016/Accepted: 27 November 2016/Published Online: 5 January 2017

Introduction

Fourier transform ion cyclotron resonance mass spectrometry (FT-ICR MS) offers unique advantages in many research fields, including proteomics [1–3], metabolomics [3, 4], and others [3], because of its high resolving power and mass accuracy for improved structural analysis. However, one limitation of the technique stems from the relatively longer signal acquisition time required to obtain higher resolving power and mass accuracy. The resolving power can be estimated by simple approximation $R = T\omega_+/4\pi$ where R is resolving power, ω_+ is measured cyclotron frequency, and t is the required signal acquisition duration [5, 6]. Therefore, one approach to decrease required signal analysis time for high resolution mass spectral acquisition is to use stronger magnetic fields [7, 8], and

to utilize multiple detection electrodes for the analysis of harmonic signals of the fundamental frequency. Increased magnetic field and increased number of multiple detection electrodes result in increased detected frequencies and, therefore, increase the achieved resolving power for signal acquisition of the same duration. In recent years, FTICR-MS instruments equipped with 21 T were developed at National Labs [9] and [10] and ICR cell designs with multiple electrodes have been demonstrated to enhance harmonic signals and improve acquisition rates [7, 11–14]. In addition, the use of multiple high resolution mass analyzers that can be operated in parallel was recently introduced as a complementary approach to help address this limitation [15]. In that work, multiple mass analyzers were aligned with the central magnetic field axis and trapped ion populations were sequentially filled in each cell in the array (up to five cells were demonstrated). Once the array was fully populated, all trapped ions were excited and detected at the same time so that five spectra could be acquired during the time required for only a single acquisition event. This approach enabled simultaneously high resolution analysis of biomolecules across a wide mass range with improved analysis speed

Electronic supplementary material The online version of this article (doi:10.1007/s13361-016-1573-z) contains supplementary material, which is available to authorized users.

Correspondence to: James E. Bruce; e-mail: jimbruce@uw.edu

directly proportional to the number of analyzers.

In multisection ICR cells, ions are able to be drifted from cell to cell along [16–19] or perpendicularly [20–23] to the magnetic field lines. The drift ICR cells were generally used for the study of ion–molecule reaction. For example, ions in an ICR cell move freely along the magnetic field axis and are trapped in three dimensions by combined electric and magnetic fields [24, 25]. The Finnigan model 2001 FTMS and the Nicolet model 2000 FTMS spectrometers [26] employed dual ICR cells and were based on the concept of ion-drift along the magnetic field lines. In those systems, the dual ICR cell was aligned with the magnetic field, differentially pumped, and ions were generated in the high-pressure “source” cell and then transferred to the low-pressure “analyzer” cell for detection. These systems were not designed for parallel acquisition and were intended to benefit from a higher pressure cell for improved ion–molecule reactions and a lower pressure cell for improved ICR signal detection that could be implemented within a single superconducting magnet. In a similar concept, but based on the capability of cross-field drift of ions, Wronka and co-workers developed a drift ICR cell whereby ions could be generated in a higher pressure cell and drifted to a lower pressure ICR cell within a single electromagnet-based system. The Ridge group drift cell consisted of ion source, analyzer, and ion collector regions [20]. Recently, Nagornov et al. also demonstrated the ability to trap ions in ICR cells and vary the position of the ion cloud prior to ion excitation. Small DC voltages were applied to detection and excitation electrodes to move ions off the central axis and decrease the contribution of magnetron motion to detected signals [27].

Although linear ICR cell arrays offer potential to expand the number of detectors to five or even more if detector size is further decreased, the possibility to expand further along the magnetic field axis is limited by available high field region within current magnet designs. However, the possibility to drift ions across the magnetic field axis offers the potential to develop non-linear ICR cell arrays and, thus, the number of detectors in an array can potentially be greatly increased. The study presented here illustrates our efforts to investigate cross-magnetic field drift to evaluate its potential use in parallel ICR signal acquisition. These results were achieved with a novel dual cell design with cells arranged relative to one another in a direction orthogonal to the central magnetic field axis. Cross-field drift was found to be useful for efficient transfer of ions from a cell located on the field axis after their accumulation to a neighboring cell off the central axis. Filling both cells and use of a single excitation and detection event showed successful parallel spectral acquisition within this orthogonal dual cell array.

Experimental

LTQ FT-ICR MS

A hybrid linear ion trap Fourier transform ion cyclotron resonance mass spectrometry (LTQ FT-ICR MS; Thermo

Scientific, Bremen, Germany) equipped with a 7 T actively shielded superconducting magnet (Oxford Nanoscience, Oxon, UK) was used to acquire all experimental data. The LTQ FT-ICR MS was modified with an orthogonal ICR cell array, a preamplifier array, a custom multi-pin feedthrough flange on the source side of the vacuum system and wiring after the removal of a cylindrical Ultra ICR cell that was originally equipped with the system. After installation, the system was pumped and baked out overnight. For ion formation, electrospray ionization (ESI) was used as an ion source with syringe pump infusion of samples at a rate of 3.0 $\mu\text{L}/\text{min}$. A spray voltage of 4.5 kV was applied to a sample solution through a metal union for ionization. The ions were injected into the LTQ for initial accumulation and were then transferred into the ICR cell array through the original equipment octapole ion guide. Ion populations inside the LTQ were accumulated with automatic gain control (AGC) on and set to 1.0×10^5 . The pressure indicated on the ion gauge in the cell region during all experiments was approximately 0.4×10^{-10} Torr.

ICR Cell Array Design

The initial design of an orthogonal dual ICR cell array used here had two independent cells in which one cell (master cell) was positioned on the central magnetic field axis and another (slave cell) beside it as illustrated in Figure 1. Except for detection electrodes, which were constructed with copper wires [28], all electrodes in this ICR cell were constructed with six identical printed circuit boards (PCBs) using gold-coated copper including two excitation plates, two drift plates, and front/back lens plates as shown in Figure 2. The excitation plates shown in Figure 2a and b were segmented into two sections; one was used for the master cell and another was used for the slave cell. Each section had five segments. The middle segments were used as excitation electrodes for master and slave cells. The length and width of the excitation electrodes were 1.8" and 0.5", respectively. The segments next to the excitation electrodes were 0.1" in width and were used as trapping electrodes. The segments next to the trapping electrodes were 0.25" in width and were held at a ground potential in all experiments. Figure 2c and d show the drift plates and the five segments used on each plate. The middle segment in each drift plate was used as a drift electrode to transfer ions from a master cell to a slave cell by applying DC voltages to these electrodes. The segments next to the drift electrodes were used as trapping electrodes. The segments next to the trapping electrodes were held at ground potential in all experiments. The front/back lens plates were segmented into two electrodes; entrance/exit lens electrodes for a master cell and front/back lens electrodes for a slave cell, as shown in Figure 2e. The entrance/exit lens electrodes had a 0.2" diameter hole at the center of the electrode through which the transferred ions from LTQ came into the master cell. To form the orthogonal ICR cell array shown in Figure 2f, excitation and drift plates were soldered to front and back lens plates. After that, 24 AWG copper wires inserted into the holes for copper wire detection electrodes shown in

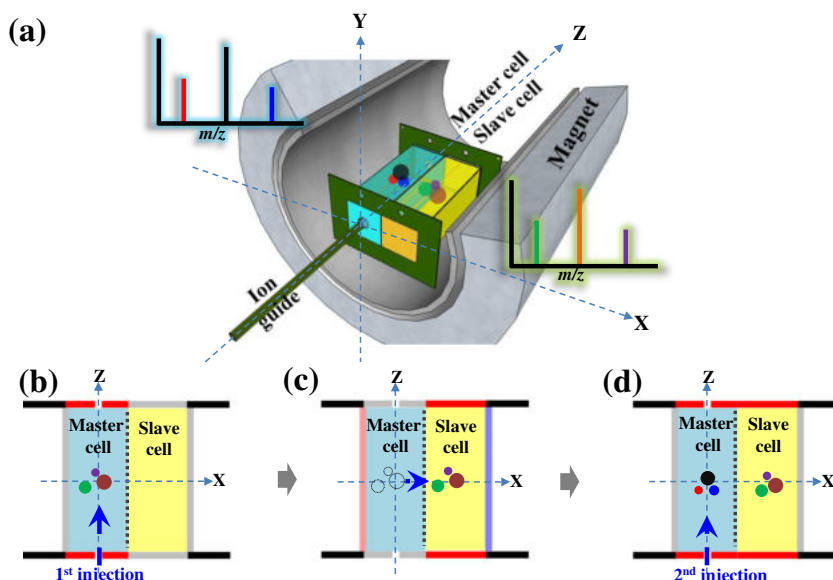


Figure 1. An orthogonal ICR cell array **(a)**. A master cell was positioned on the central magnetic field axis and a slave cell beside it. To obtain parallel mass spectra, ions from LTQ were trapped in the master cell **(b)**, and then the trapped ions were transferred to the slave cell by applying drift voltages to drift electrodes for cross-field drift of ions **(c)**. The next transferred ions from LTQ were injected to the recently vacated master cell **(d)**. After filling the two cells, the trapped ions were excited and detected in parallel

Figure 2e were soldered to the cell array. Figure 2g shows the orthogonal ICR cell array with the removal of the drift plates to reveal the copper wires used as detection electrodes, which were placed above the excitation electrodes (0.1" away from the electrodes). The trapping electrode segments were electrically coupled together by soldering 22 AWG copper wires on the pads on a cell outer surface to make trapping electrodes. The solder used for the ICR cell was 99.3/0.7 Sn-Cu lead-free solder alloy. The entire length of the orthogonal ICR cell array was 2.54". All individual PCB components for preparing an orthogonal ICR cell array were designed using a circuit board

layout program EAGLE ver. 7.3.0 (CadSoft Computer, Pembroke Pines, FL, USA) and manufactured by OSH Park (Advanced Circuits, Aurora, CO, USA).

The assembled ICR cell array was placed at the end of the octapole ion guide in the place of the ThermoFisher Ultra ICR cell. The detection electrode pairs from each cell were connected to a custom vacuum-compatible preamplifier array (GAA Custom Engineering), which was mounted at 0.6" away from the front lens plate of the orthogonal ICR cell array, by using Kapton-coated wires (22 AWG; Accu-Glass Products, Inc. Valencia, Ca, USA) to allow parallel ICR signal amplification.

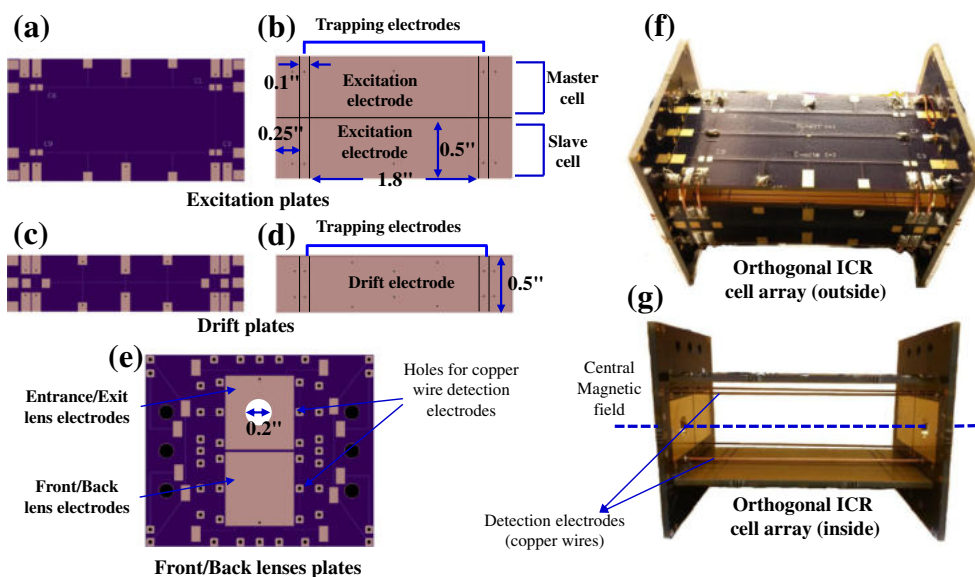


Figure 2. Individual PCB components and assembled drift ICR cell array. Excitation plate outer surface **(a)** showing pads and inner surface **(b)** showing excitation and trapping electrodes printed on board. Drift plate outer surface **(c)** and inner surface **(d)**. Front and back lenses plates **(e)**. Drift ICR cell array assembly outside **(f)** and inside **(g)** showing copper wires used as detection electrodes

The preamp array consisted of three single preamplifiers [15], although for this work only two preamplifiers were used.

To populate both cells in the orthogonal cell array, trapping and drift voltages applied to each electrode were independently controlled with a multi-channel programmable DC power supply (Modular Intelligent Power Source (MIPS), GAA Custom Engineering, Benton City, WA, USA) [15]. Figure 3 shows the DC voltage profiles used to trap and drift ions for the orthogonal dual cell array. In this graph, the black color trace indicates the DC voltage changing with time for a LTQ back lens electrode. The purple color traces indicate the DC voltages changing with time for the master's front/back trapping electrodes. The red color traces indicate the time-dependent DC voltages applied to the drift electrodes. The green color traces indicate the time-dependent DC voltages applied to the slave's front/back trapping electrodes. To trap ions in both cells, the first population of ions transferred from the LTQ was injected into a master cell by applying a negative voltage to the master's front trapping electrode and a positive voltage to the master's back trapping electrode. To trap the ions in the master cell, the negative voltage applied to the master's front trapping electrode was switched to a positive voltage, but the positive voltage applied to the master's back trapping electrode remained constant (A). The trapped ions were then drifted to the slave cell by applying small positive and negative voltages to two drift electrodes for a few milliseconds (B). The drifted ions were trapped in the slave cell by applying a positive voltage to the slave's front/back trapping electrodes that were kept until detection (C). Finally, the second transferred ions from LTQ were injected to the vacated master cell by applying a negative voltage to the master's front trapping electrode and a positive voltage to the master's back trapping electrode. To trap the ions in the master cell, the applied positive voltage to the back trapping electrode remained constant, and the negative voltage to the front trapping electrode was switched to a

positive voltage (D). The entrance/exit and front/back lens electrodes were simultaneously controlled with each front/back trapping electrode to inject and trap ions in the cells in all experiments. After filling both cells, cyclotron motion of trapped ions in both cells was excited simultaneously with the waveform amplitude of 0.1 (ThermoFisher Excalibur software) applied to both cells, and then ICR signals were detected after gradually decreased trapping voltages (E). Parallel ICR signals from both cells were simultaneously amplified using the independent preamplifier array that was connected to the detection electrodes of each cell. Each amplifier output signal was connected to a single vacuum feedthrough pin with kapton-coated wire and then to a Saleae digitizer (Logic 8; Saleae Inc., South San Francisco, CA, USA). The number of samples and sample rate were set to 131072 and 781250, respectively. DC power (± 2.5 V) to operate the in-vacuum preamplifier was supplied by an external power supply. The digitized time domain signals were transferred to a computer through a USB interface and processed with ICR-2LS (<http://omics.pnl.gov/software/icr-2ls>).

Sample Preparation

All peptides and Ultramark 1621 (a mixture of fluorinated phosphazenes) were purchased from Sigma (St. Louis, MO, USA). HPLC grade methanol and acetic acid were obtained from Fisher Scientific (Pittsburgh, PA, USA). Ten μM standard peptide solutions were prepared by dissolving them in 1:1 (v/v) water/methanol solvent mixtures containing 0.1% (v/v) of acetic acid. An Ultramark 1621 stock solution was prepared by dissolving 10 μL of Ultramark 1621 in 10 mL of acetonitrile. A 10 mL solution of Ultramark 1621 was prepared by dissolving 100 μL of the stock solution of Ultramark 1621 in a solution of 1% acetic acid in 50:50 methanol:water.

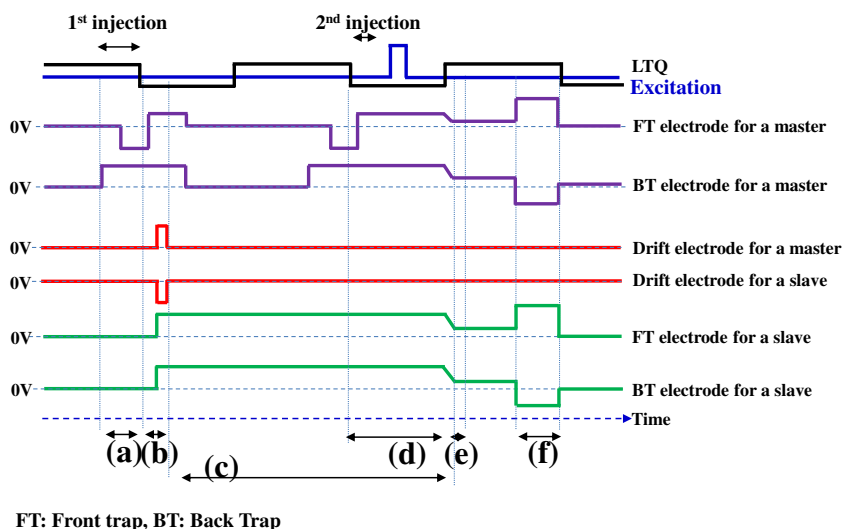


Figure 3. DC voltage profiles produced by MIPS to independently control DC voltage to trap ions in each cell. (a) Inject and trap ions in a master cell, (b) drift ions from the master cell to a slave cell, (c) trap the drifted ions in the slave cell until detection. (d) Inject and trap ions in the vacated master cell, (e) ICR signals detection, and (f) quench

Result and Discussion

Characterization of Drift Voltages and Transfer Event Duration

The unique orthogonal dual ICR cell array developed in this work allows characterization of the cross-magnetic field drift process by measurement of ions in either cell as a function of the parameters, drift time and drift electrostatic field. Both parameters were investigated to identify optimal values used for subsequent studies using a 10 μM solution of Ultramark 1621. For this experiment, optimized trapping potentials of -6 V and $+4$ V were applied to the master cell front and back trapping electrodes, respectively, during injection of ions. After ion injection, the applied voltages were switched to $+4$ V on both electrodes to trap ions in the master cell. The trapped ions were drifted by applying drift voltages and trapped in a slave cell by applying an optimized trapping potential ($+4$ V) to the slave cell simultaneous with the drift voltages. After drift of ions, cyclotron motion of trapped ions was excited simultaneously with the waveform amplitude of 0.1, and then ICR signals were detected with a decreased trapping voltage ($+3$ V). To identify the optimal drift voltages and drift time, the peak

intensities of the base peak observed in both cells were measured during drift voltage and time variations. For characterization of drift voltages, the voltage applied to the master cell drift electrode ($V_{\text{de}1}$) was varied over the range from 0 to $+2.0$ V for fixed $V_{\text{de}2} = -0.2$ V. The duration of drift potential applications was 1.5 ms. From each experimental condition, mass spectra from both cells were obtained four times and the standard deviation of measured peak intensities was calculated. Figure 4a shows that increasing the difference between the applied drift potentials increases the measured peak intensity obtained from the slave cell until $+1.7$ V, and decreases the peak intensity obtained from the master cell from $+0.8$ V. Further increase of the difference in drift potential difference ($\Delta V_{\text{de}1-\text{de}2}$) by increasing $V_{\text{de}1}$ beyond 1.7 V resulted in decreased slave cell peak intensities. To further investigate drift voltage dependencies, the applied drift voltages ($V_{\text{de}1}$) were varied in the range from 0 to $+2.0$ V for different fixed $V_{\text{de}2} = -0.5$ V, -1.5 V, -2.5 V, and -4.5 V. Figure 4b shows that as $V_{\text{de}2}$ is made more negative, a lower drift voltage ($V_{\text{de}1}$) was observed to be required for optimum slave cell peak intensity. Moreover, the observed optimum signals appear much more sensitive to $V_{\text{de}1}$ changes compared with $V_{\text{de}2}$ changes because

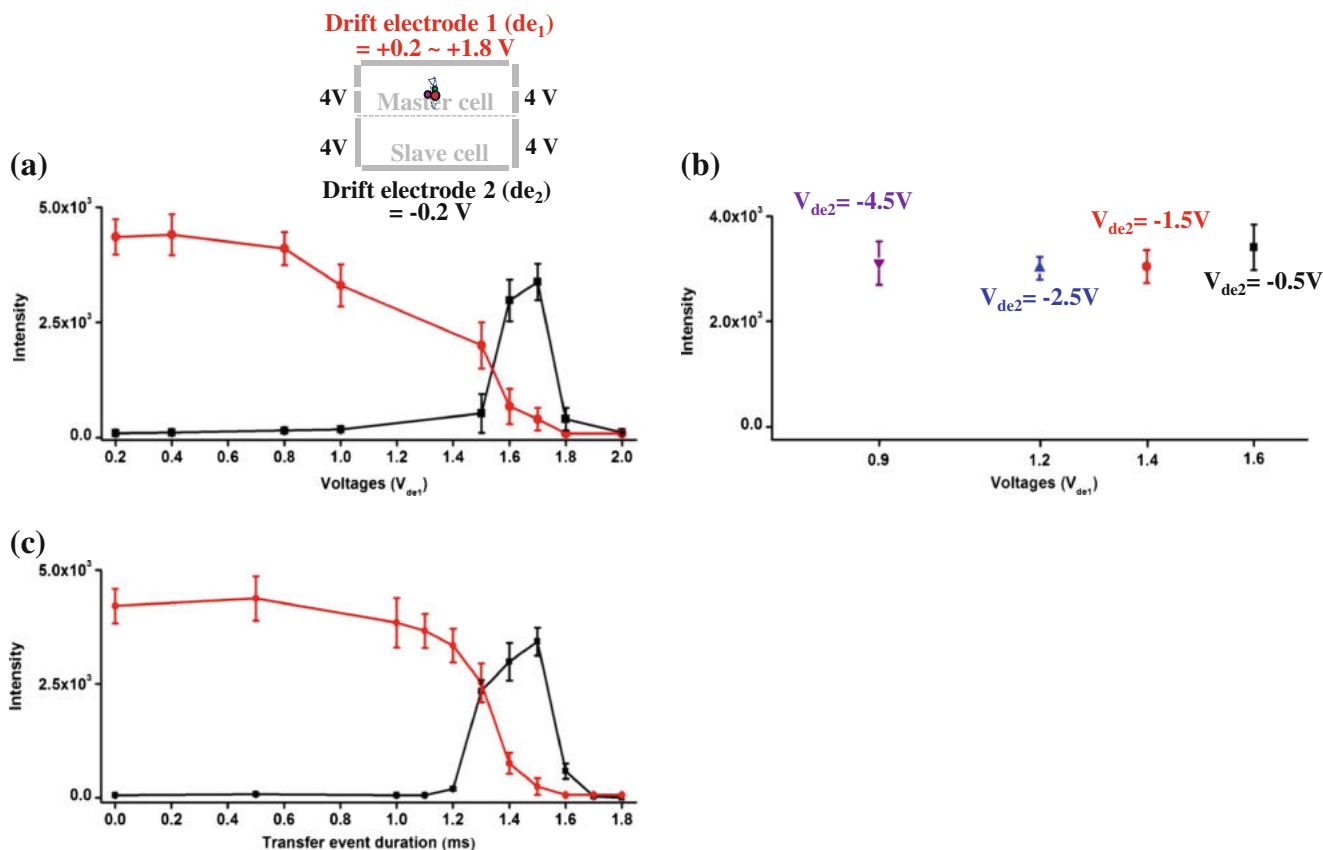


Figure 4. Characterization of drift voltages and transfer event duration. **(a)** $V_{\text{de}1}$ was varied in the range from $+0.2$ to $+1.8$ V for a fixed $V_{\text{de}2} = -0.2$ V, and **(b)** derived optimum $V_{\text{de}1}$ for different fixed $V_{\text{de}2} = -4.5$ V, -2.5 V, -1.5 V, and -0.5 V to obtain the most abundant peak intensity in the slave cell (transfer time = 1.5 ms). **(c)** The duration of the drift event was investigated for the drift voltages ($V_{\text{de}1} = +1.7$ V and $V_{\text{de}2} = -0.2$ V) applied at 3.5 ms after a $+4$ V trapping voltage was applied to a master cell to trap ions. Applied drift voltages remained constant for transfer event duration as shown

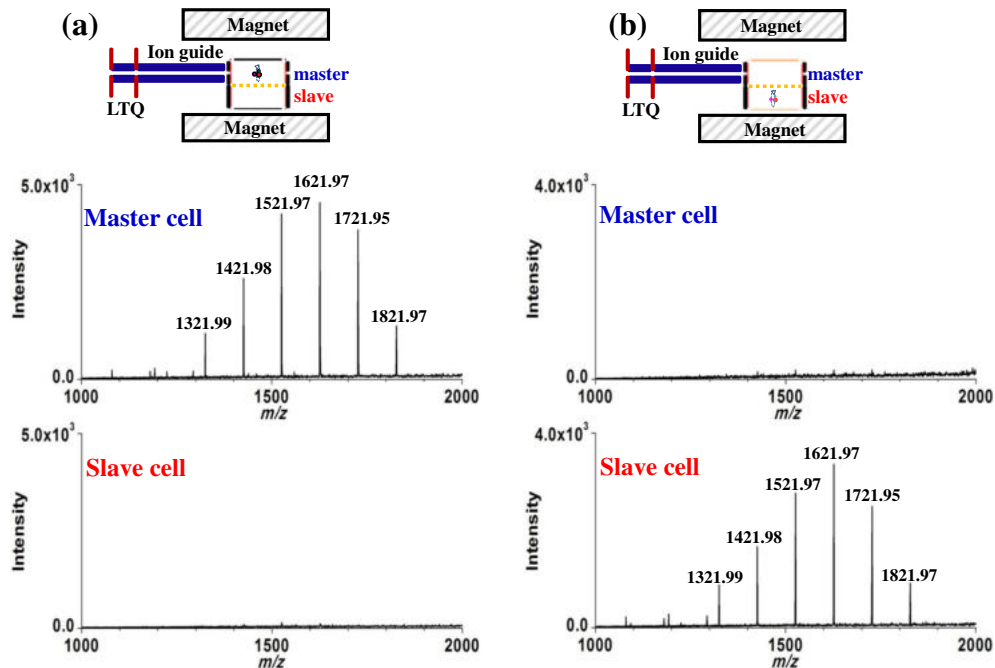


Figure 5. Parallel mass spectra obtained from both cells at the same time before (a) and after (b) drift of ions by applying DC voltages to drift electrodes to transfer ions from a master cell to a slave cell. Prior to trapping ions to investigate independent function of the slave cell, the drift ICR cell was quenched to remove any residual ions from the previous measurement

the ion cloud trapped in the master cell is initially closer to V_{de1} than V_{de2} . The effective potential experienced by the ions should decrease by roughly the square of the distance between the ions and the electrode [29].

To optimize transfer event duration, drift voltages ($V_{de1} = +1.7$ V and $V_{de2} = -0.2$ V) were applied to the drift electrodes

at 3.5 ms after a +4 V trapping voltage was applied to the master cell front trapping electrode to trap ions. During ion drift, applied drift voltages remained constant for various time durations (0 to 1.8 ms). Figure 4c shows the observed variation of measured base peak intensity as a function of transfer event duration. Increasing the transfer event duration increased the

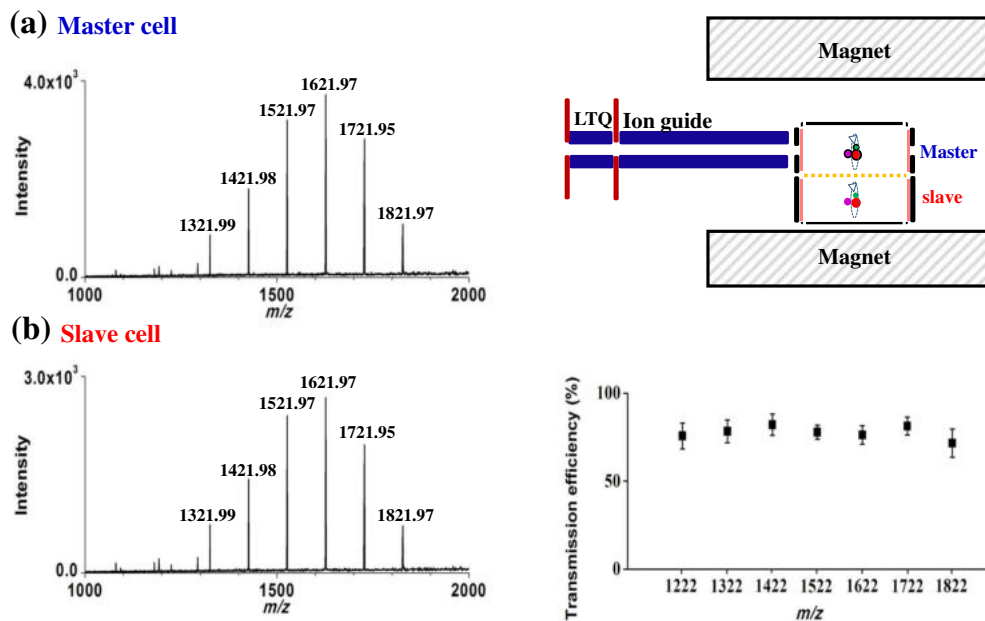


Figure 6. Parallel detection of equivalent ion populations using calibration. Master (a) and slave (b) cells were filled with equivalent ions. All ions were simultaneously excited, ion signals were amplified, recorded, and processed to yield parallel spectral acquisition in a drift ICR cell array

Table 1. Calculated Mass Error for Each Peak Observed from Both Cells

Theoretical m/z	Theoretical frequency (Hz)	Measured m/z	Measured frequency (Hz)	Calibrated m/z	ppm
Master cell					
1321.9843	81837.6282	1322.9674	81776.8713	1321.9863	1.6
1421.9779	76082.2120	1423.0419	76025.3061	1421.9798	1.4
1521.9715	71083.0576	1523.1511	71027.9544	1521.9744	1.2
1621.9651	66700.2961	1623.2642	66646.8706	1621.9670	1.2
1721.9587	62826.5458	1723.4366	62772.6537	1721.9520	-1.6
Slave cell					
1321.9843	81837.6340	1323.0446	81772.1048	1321.9864	1.9
1421.9779	76082.2149	1423.1392	76020.1098	1421.9806	1.7
1521.9715	71083.0580	1523.2313	71024.2162	1521.9691	-1.6
1621.9651	66700.2943	1623.3892	66641.7309	1621.9673	1.4
1721.9587	62826.5420	1723.5304	62769.2346	1721.9554	-1.9

number of drifted ions to a slave cell, but decreased the number of ions in the master cell. With transfer duration of 1.5 ms or greater, decreased the slave cell base peak intensity was observed.

Parallel Mass Spectra with and Without Drift Voltages

To confirm independent function of slave and master cells, ICR signals were obtained from both cells at the same time with and without drifting a trapped ion population from master to slave cells. To test master cell performance, the ions from LTQ were trapped in the master cell by applying the trapping voltage (+4 V) to the master cell front/back trapping electrodes. During these steps, the slave cell front/back trapping electrodes and drift electrodes were kept at 0 V. After the ions were trapped in the master cell, rf voltage was applied to the excitation electrodes for both cells to excite ion cyclotron motion and ICR signals from each cell were acquired. Figure 5 shows the resulting mass spectra. As shown in Figure 5a, expected abundant ion signals from Ultramark 1621 were observed in the

master cell, but no peaks were detected in the slave cell. To further test independent function of the master cell, a +4 V trapping voltage was simultaneously applied to the slave cell with the trapping voltage applied to trap ions in the master cell, and the applied trapping voltages to both cells were decreased to +3 V for detection. Although the trapping voltage (+4 V) was applied to the slave cell during trapping ions in the master cell, no peaks were detected in the slave cell without application of the ion drift event.

Prior to trapping ions to investigate independent function of the slave cell, the ICR cell was quenched to remove any residual ions from the previous measurement and then ions from LTQ were trapped in the master cell by applying a +4 V trapping voltage, as above. The trapped ions were then drifted to the slave cell by application of optimized drift voltages ($V_{de1} = +1.7$ V and $V_{de2} = -0.2$ V for 1.5 ms) and simultaneously, a +4 V trapping voltage was applied to the slave cell front and back trapping electrodes before cyclotron excitation. After the ion drift event, 0 V was applied to the master cell front and back trapping electrodes. After ion excitation, the applied slave cell trapping voltages were decreased to +3 V and ICR signals from

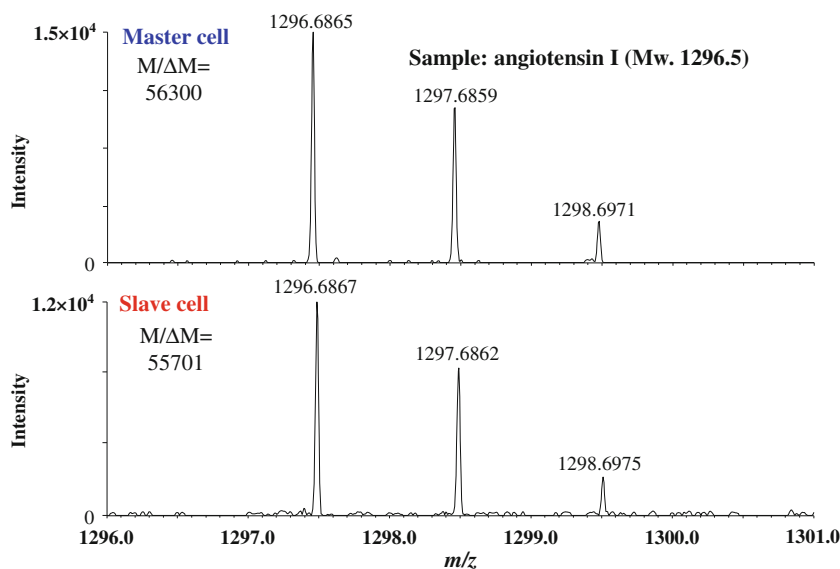


Figure 7. High resolution spectra of the peptide angiotensin I showing resolving power $R(\text{FWHM})$ of nearly 60,000 in both cells

both cells were acquired in parallel. The resulting mass spectra (Figure 5b) acquired with 0 V applied to the master cell after drift of ions show reversed results; no ion signals observed in the master cell, but ion signals were detected in the slave cell. Additionally, experiments performed where +4 V trapping voltages were maintained on master cell trapping electrodes after the ion drift event produced similar results: ions signals in the slave cell, no ion signals in the master cell.

Parallel Detection of Equivalent Ion Populations

To demonstrate parallel detection of equivalent ion populations, the first accumulated population of ions in the LTQ was trapped in the master cell by applying a +4 V trapping voltage. Trapped ions were drifted to a slave cell by applying drift voltages ($V_{de1} = +1.7$ V and $V_{de2} = -0.2$ V for 1.5 ms) and then trapped in the slave cell by applying +4 V to its trapping electrodes. After drifting trapped ions to the slave cell, a second population of ions was accumulated in the LTQ, injected, and trapped in the vacated master cell by applying a trapping voltage (+4 V). After ion populations were trapped in both cells, a single cyclotron excitation waveform was applied to excitation electrodes in both cells simultaneously. After excitation, the trapping voltages applied to both cells were decreased to +3 V and the ICR signals from both cells were acquired in parallel. The resulting mass spectra and corresponding time domain signals (transients) are shown in Figure 6 and Supporting Information (Supplementary Figure S-1). After drift of ions, no obvious discrimination in S/N and intensity variations observed between master and slave cells resultant from cross-magnetic field drift used for ion transfer. The transmission efficiency for ions between $m/z = 1000$ to 2000

estimated by (the peak intensity from the slave cell/the peak intensity from the master cell) $\times 100$ is 75% or higher.

Calibration and Mass Accuracy

To perform mass calibration for each cell with external calibration, equivalent populations of Ultramark ions were trapped in both cells and parallel ICR signals were acquired for 0.3 s. The trapping potentials applied to both cells for cyclotron excitation were +4 V and +3 V for signal acquisition. Applied ion drift voltages were $V_{de1} = +1.7$ V and $V_{de2} = -0.2$ V for 1.5 ms as described above. Calibration for both cells was accomplished with a two-parameter calibration equation, $m/z = A/f + B/f^2$ [5, 30]. In this equation, the A term is related to magnetic field strength and the B term related to magnetron motion and the electric field generated primarily from trapping potentials, and f is the measured cyclotron frequency. To calculate the appropriate mass calibration parameters, the equation was rewritten as $f \times m/z = A + B/f$ and the observed peaks were mapped on $f \times m/z$ versus $1/f$ plots as shown in Supporting Information (Supplementary Figure S-2). The plots show that the points fit linear equations, from which A and B parameters of the calibration equation for each cell are obtained; $A = 108,199,088.25$ and $B = -902,890,884.58$ for the master cell, and $A = 108,199,142.79$ and $B = -906,722,854.42$ for the slave cell. After calibrating the observed ion peaks in each cell by the calibration equation, the mass measurement accuracies were calculated for the Ultramark 1621 ion peaks and are shown in Table 1, and mass measurement error values on the order of 1 ppm were obtained from both cells in the orthogonal dual ICR cell array.

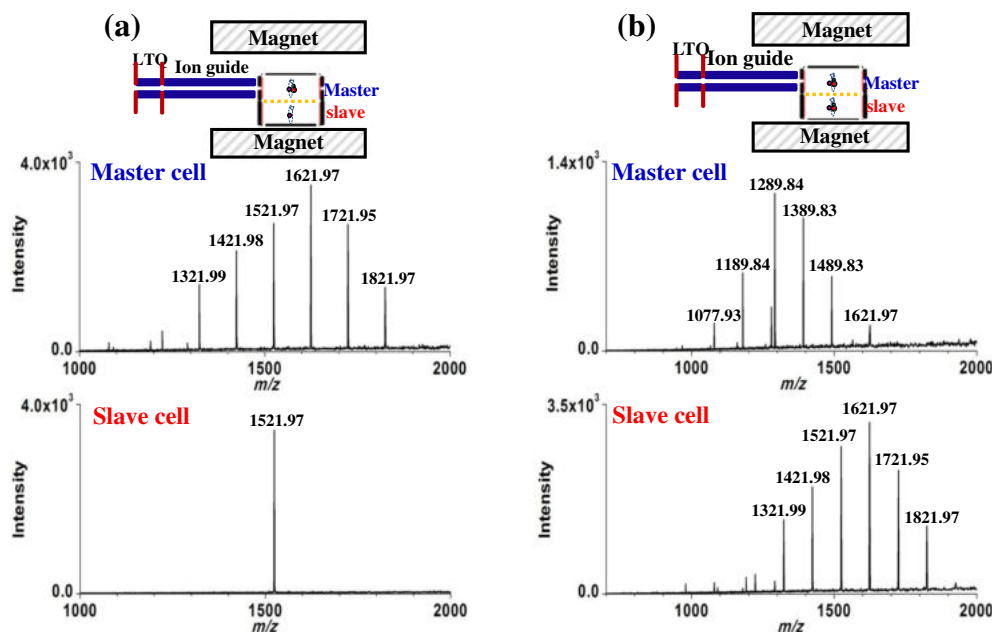


Figure 8. Multiple injections of different ion populations. **(a)** All ions (m/z 1000–2000) accumulated in the LTQ were injected into the master cell and ion at m/z 1522 was selected and injected into slave cell. **(b)** The fragmented ions for the selected ion at m/z 1622 in LTQ were transferred to a master cell and the accumulated ions in the LTQ were transferred to a slave cell for full MS analysis

Revolving Power

One question regarding the use of multiple cells positioned orthogonal to the magnetic field axis relates to whether parallel, stable ICR signals can be generated in both cells where the ICR orbit center in the slave cell is removed from the magnetic field central axis. If positioning the ions in the slave cell is not compatible with stable, coherent cyclotron motion, high resolution spectral acquisition would be precluded. To investigate resolving power of this orthogonal cell configuration, mass spectra from both cells were evaluated with the analysis of the peptide angiotensin I (MW = 1296.5). The trapping voltage applied to both cells was +4 V, and the applied ion drift conditions used to transfer ions to the slave cell were $V_{de1} = +1.7$ V and $V_{de2} = -0.2$ V for 1.5 ms. All voltages used to inject, trap, drift, and eject ions were the same as described above. Figure 7 shows resulting mass spectra acquired by accumulation and injection of equivalent angiotensin ion populations for excitation and detection in either master or slave cells. Thus, to at least the level of moderately high resolving power that would be acquired during on-line liquid chromatography separation of proteome samples, the performance of orthogonal cells can help further increase the number of detectors available in a mass spectrometer array. Future efforts will investigate additional orthogonal cells and further refined cell geometries to provide additional benefits.

Multiple Injections of Different Ion Populations

One benefit demonstrated previously for a cell array [15] is that each cell can be used to detect different ion populations. To test this capability with the orthogonal dual cell array, two different ion populations were accumulated in each cell in the array (Figure 8). For these experiments, ions from different mass ranges or different ion types were selected or produced in the LTQ, transferred to selected cells, and parallel ICR signals were acquired. AGC target values for the FT analyzer were set to 5.0×10^6 , 6.0×10^5 , and 8.0×10^5 for the full MS target, the SIM target, and MSⁿ target, respectively. The spectra in Figure 8a show results of multiple injections of differing ion populations in each cell. For this experiment, full MS analysis was performed in the master cell, whereas the slave cell was used to trap and detect only selected ions at $m/z = 1522$. As shown in Figure 8a, a distribution of Ultramark ions and single peak were observed in the master cell and the slave cell, respectively. Figure 8b shows simultaneous acquisition of MS and MS/MS spectra of Ultramark ions. In this case, the full distribution of Ultramark ions was transferred and detected in the slave cell, while fragment ions from the Ultramark species near $m/z = 1622$ were transferred to and detected in the master cell. These results illustrate that orthogonal cells can be used to provide parallel detection of independent mass ranges or independent stages of mass analysis. These capabilities can further increase the number and type of measurements that can be performed during chromatographic separations.

Conclusions

FT-ICR MS is a powerful instrument for the study of complex biological samples because of its ability to acquire high performance measurements; however, this typically requires longer signal acquisition times to achieve high resolution. One approach to decrease required signal analysis time for high resolution mass spectral acquisition is to use multiple high resolution mass analyzers [15]. In this study, we developed a new multiple mass analyzer called an orthogonal dual ICR cell array that consists of master and slave cells. The master cell was positioned on the central magnetic field axis with the slave cell positioned immediately adjacent to the master cell. To obtain parallel ICR signals, ions were trapped in both cells by independently controlling the applied voltages to trapping and drift electrodes. After filling both cells, a common rf waveform was applied to the excitation electrodes of both cells and ICR signals were acquired in parallel. With the current orthogonal ICR cell array, no obvious discrimination in S/N and intensity variations were observed between master and slave cells as a result of cross-magnetic field drift used for ion transfer. The observed transmission efficiency between cells for all ions was 75% or higher. High resolution spectra (60,000 FWHM) were observed to be achievable with either the master cell or slave cell. This study shows that the capability of cross-field drift of ions can be used to transfer ions with nonlinear multiple mass analyzers and potentially extend the number of ICR cells beyond those possible with linear arrays. Taken together with our previously reported linear five-cell array technology [15], the present results suggest that parallel acquisition of 10 or more spectra is possible with a two- or three-dimensional ICR cell array.

Acknowledgments

This work was supported by the National Institutes of Health through grant 5R01GM097112.

References

1. Bantscheff, M., Lemeer, S., Savitski, M., Kuster, B.: Quantitative mass spectrometry in proteomics: critical review update from 2007 to the present. *Anal. Bioanal. Chem.* **404**, 939–965 (2012)
2. Yates, J.R., Ruse, C.I., Nakorchevsky, A.: Proteomics by mass spectrometry: approaches, advances, and applications. *Annu. Rev. Biomed. Eng.* **11**, 49–79 (2009)
3. Griffiths, W.J., Wang, Y.: Mass spectrometry: from proteomics to metabolomics and lipidomics. *Chem. Soc. Rev.* **38**, 1882–1896 (2009)
4. Courant, F., Antignac, J.-P., Dervilly-Pinel, G., Le Bizec, B.: Basics of mass spectrometry based metabolomics. *Proteomics* **14**, 2369–2388 (2014)
5. Marshall, A.G., Hendrickson, C.L., Jackson, G.S.: Fourier transform ion cyclotron resonance mass spectrometry: a primer. *Mass Spectrom. Rev.* **17**, 1–35 (1998)
6. Amster, I.J.: Fourier transform mass spectrometry. *J. Mass Spectrom.* **31**, 1325–1337 (1996)
7. Nagornov, K.O., Gorshkov, M.V., Kozhinov, A.N., Tsybin, Y.O.: High-resolution Fourier transform ion cyclotron resonance mass spectrometry with increased throughput for biomolecular analysis. *Anal. Chem.* **86**, 9020–9028 (2014)

8. Scigelova, M., Hornshaw, M., Giannakopoulos, A., Makarov, A.: Fourier transform mass spectrometry. *Mol. Cell. Proteom.* **10**, (2011)
9. Hendrickson, C.L., Quinn, J.P., Kaiser, N.K., Smith, D.F., Blakney, G.T., Chen, T., Marshall, A.G., Weisbrod, C.R., Beu, S.C.: 21 Tesla Fourier transform ion cyclotron resonance mass spectrometer: a national resource for ultrahigh resolution mass analysis. *J. Am. Soc. Mass Spectrom.* **26**, 1626–1632 (2015)
10. Shaw, J.B., Lin, T.-Y., Leach, F.E., Tolmachev, A.V., Tolić, N., Robinson, E.W., Koppenaal, D.W., Paša-Tolić, L.: 21 Tesla Fourier transform ion cyclotron resonance mass spectrometer greatly expands mass spectrometry toolbox. *J. Am. Soc. Mass Spectrom.* 1–8 (2016)
11. Misharin, A.S., Zubarev, R.A.: Coaxial multi-electrode cell ('O-trap') for high-sensitivity detection at a multiple frequency in Fourier transform ion cyclotron resonance mass spectrometry: main design and modeling results. *Rapid Commun. Mass Spectrom.* **20**, 3223–3228 (2006)
12. Misharin, A.S., Zubarev, R.A., Doroshenko, V.M.: Fourier transform ion cyclotron resonance mass spectrometer with coaxial multi-electrode cell ('O-trap'): first experimental demonstration. *Rapid Commun. Mass Spectrom.* **24**, 1931–1940 (2010)
13. Nikolaev, E.N., Rakov, V.S., Futrell, J.H.: Analysis of harmonics for an elongated FTMS cell with multiple electrode detection. *Int. J. Mass Spectrom. Ion Process.* **157/158**, 215–232 (1996)
14. Vorobyev, A., Gorshkov, M.V., Tsybin, Y.O.: Towards data acquisition throughput increase in Fourier transform mass spectrometry of proteins using double frequency measurements. *Int. J. Mass Spectrom.* **306**, 227–231 (2011)
15. Park, S.-G., Anderson, G.A., Navare, A.T., Bruce, J.E.: Parallel spectral acquisition with an ion cyclotron resonance cell array. *Anal. Chem.* **88**, 1162–1168 (2016)
16. Wobschall, D.: Ion cyclotron resonance spectrometer. *Rev. Sci. Instrum.* **36**, 466–475 (1965)
17. Miasek, P.G., Beauchamp, J.L.: A novel trapped-ion mass spectrometer for the study of ion-molecule reactions. *Int. J. Mass Spectrom. Ion Phys.* **15**, 49–66 (1974)
18. Hunt, D.F., Shabanowitz, J., McIver, R.T., Hunter, R.L., Syka, J.E.P.: Ionization and mass analysis of nonvolatile compounds by particle bombardment-quadrupole-Fourier transform mass spectrometry. *Anal. Chem.* **57**, 765–768 (1985)
19. Alford, J.M., Williams, P.E., Trevor, D.J., Smalley, R.E.: Metal cluster ion cyclotron resonance. Combining supersonic metal cluster beam technology with FT-ICR. *Int. J. Mass Spectrom. Ion Process.* **72**, 33–51 (1986)
20. Wronka, J., Strobel, F., Ridge, D.P.: Adaptation of an ICR drift cell for tandem ICR. *Int. J. Mass Spectrom. Ion Process.* **71**, 303–307 (1986)
21. Heninger, M., Fenistein, S., Durup-Ferguson, M., Ferguson, E.E., Marx, R., Mauclaire, G.: Radiative lifetime for $v = 1$ and $v = 2$ ground state NO^+ ions. *Chem. Phys. Lett.* **131**, 439–443 (1986)
22. Mauclaire, G., Heninger, M., Fenistein, S., Wronka, J., Marx, R.: Radiative relaxation of vibrationally excited ions. *Int. J. Mass Spectrom. Ion Process.* **80**, 99–113 (1987)
23. Mauclaire, G., Deraï, R., Fenistein, S., Marx, R.: Energy disposal in thermal-energy charge transfer reactions determined by kinetic energy measurements of product ions: $\text{Ne}^{++}\text{O}_2 \rightarrow \text{O}^{++}\text{O} + \text{Ne}$ and $\text{Ar}^{++}\text{O}_2 \rightarrow \text{O}_2^{++}\text{Ar}$. *J. Chem. Phys.* **70**, 4017–4022 (1979)
24. Mauclaire, G., Sourisseau, C.: An improved balanced drift voltage control for ion cyclotron resonance drift cells. *Int. J. Mass Spectrom. Ion Process.* **83**, 215–221 (1988)
25. Beauchamp, J.L.: Ion cyclotron resonance spectroscopy. *Annu. Rev. Phys. Chem.* **22**, 527–561 (1971)
26. Shea, R.C., Petzold, C.J., Liu, J.-A., Kenttämä, H.I.: Experimental investigations of the internal energy of molecules evaporated via laser-induced acoustic desorption into a fourier-transform ion cyclotron resonance mass spectrometer (LIAD/FT-ICR). *Anal. Chem.* **79**, 1825–1832 (2007)
27. Nagornov, K.O., Kozhinov, A.N., Tsybin, O.Y., Tsybin, Y.O.: Ion trap with narrow aperture detection electrodes for Fourier transform ion cyclotron resonance mass spectrometry. *J. Am. Soc. Mass Spectrom.* **26**, 741–751 (2015)
28. Hanson, C.D., Castro, M.E., Kerley, E.L., Russell, D.H.: Field-corrected ion cell for ion cyclotron resonance. *Anal. Chem.* **62**, 520–526 (1990)
29. Child, C.D.: Discharge from Hot CaO. *Phys. Rev. (Ser. I)* **32**, 492–511 (1911)
30. Ledford, E.B., Rempel, D.L., Gross, M.L.: Space charge effects in Fourier transform mass spectrometry. II. Mass calibration. *Anal. Chem.* **56**, 2744–2748 (1984)